
Introduction to Inverse Methods

1.1. Introduction

In the field of structural calculations, the finite elements method allows for determining a structure's physical response to an applied force. This technique not only enables us to determine the stress states on a mechanical structure's interior, but also to model the complete manufacturing processes, for example. Nowadays, the significantly reduced calculation time allows us to address so-called inverse problems. By repeating the calculations by finite elements while modifying the material's parameters or the structure's geometry, we can identify an optimal solution for the problem in question. The procedure, which couples optimization and calculations by finite elements, is of utmost importance for the manufacturing industry, for example, as this virtual development reduces the time and costs involved in developing new products.

For those who understand the difference, the terminology of “inverse problem” is used, as opposed to that of “direct problem”, to refer to solving a differential equation based on the known parameters in order to calculate the system's response. In the instance of an inverse problem, the system's response is assumed to be known. Therefore, we aim to determine the physical or geometrical parameters that, when used in direct problems, allow us to find the prescribed system's response. Inverse problems also involve an objective function to be constructed according to the application, measuring a gap between the known response and the responses obtained from the sets of different parameters by solving the direct problem. Various inverse problems can be distinguished: for example, restoring a system to its past state by knowing its current state (if this system is invariable) or

determining the system's parameters by knowing (one part of) its evolution. This last problem is that of identifying parameters, which will be dealt with in section 1.2 (see Figure 1.2).

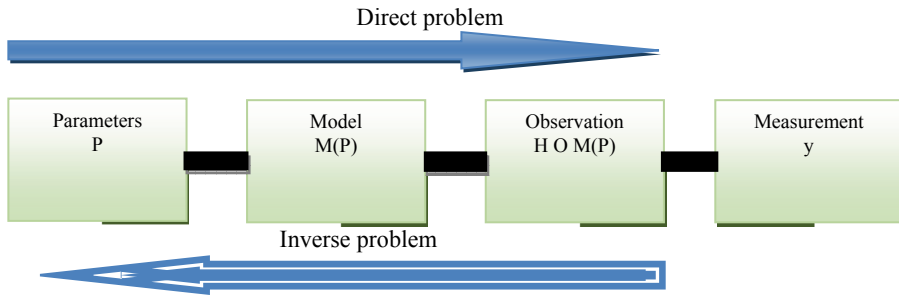


Figure 1.1. Illustration of a direct problem and its inverse problem. For a color version of this figure see, www.iste.co.uk/elhami/dynamics.zip

There are two main categories of techniques for solving an inverse problem:

1) Gradient-type techniques have often been considered in applications for which the necessary time to assess a direct problem is significant. They consist of identifying the minimum of the objective function as a point where this function's gradient cancels itself out. This approach does not guarantee that the global minimum will be identified, but it has the benefit of quickly converging toward a minimum. This minimum will be global if the initial one is close enough to the desired solution, which is quite often the case in engineering problems.

2) Stochastic [BAR 01] or progressive methods have major significance in non-differentiable optimization and are a recourse for problems, which have local minima. Gradient methods are used when the function to be optimized is differentiable. They use the information given by the partial derivatives. In the instance of differentiable functions whose convexity cannot be guaranteed, hybrid or mixed algorithms are often used to combine the advantages of stochastic algorithms and gradient algorithms. The method chosen depends on the nature of the inverse problem (differentiable, non-differentiable, etc.) and above all on the calculation time necessary for assessing the system's response.

1.2. Identification methods

In the general context of physics and particularly in solid mechanics, it is often necessary to assess or identify the physical quantities governing the system studied. In many cases, the quantities being searched for (Young's modulus, coefficient damping, etc.) may not be directly measurable and one must use other measurable quantities (accelerations, strains, speeds, etc.) to obtain more information. The principle of the identification methods consists of establishing a mathematical relation based on physical laws, also called models, so that the quantities searched for (sometimes called parameters) are found from the measurements available. Thus, from a mathematical point of view, the solution to such a problem may encounter problems relating to solutions' existence, unicity and continuity. Consequently, the identification methods can be considered to fall into the category of inverse problems where, unlike the solutions to direct problems, one must overcome the difficulty of the problem being ill-posed.

From a mechanical point of view, the reference problem that we are aiming to solve consists of studying the evolution of a structure occupying a volume in an interval of time $t \in [0, T]$ (see Figure 1.2).

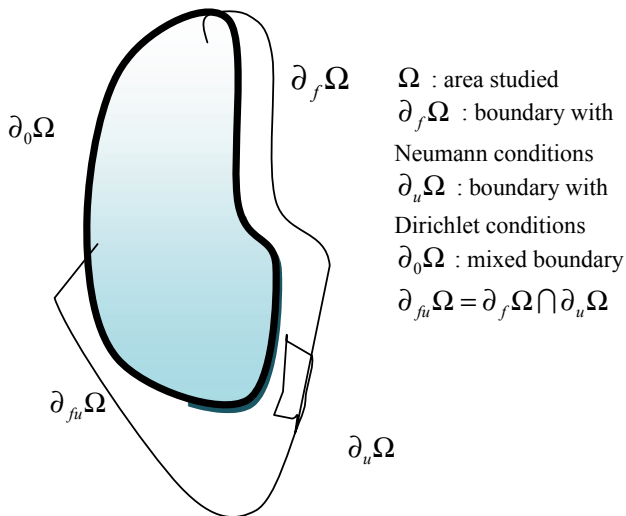


Figure 1.2. Area studied and its limits using the data available. For a color version of this figure see, www.iste.co.uk/elhami/dynamics.zip

The structural behavior is given by the solution to the reference problem defined by:

Find the displacement $u(z, t) \in U(\bar{u})$ and the stresses $\sigma(z, t) \in S(\bar{f})$
 $\forall t \in [0, T], \forall z \in \Omega$

– Behavior equation:

$$-\rho \ddot{u}(z, t) + \operatorname{div}(\sigma(z, t)) = 0 \quad [1.1]$$

– Behavioral laws:

$$\sigma(z, t) = C(\varepsilon(u(z, t)), \theta) \quad [1.2]$$

where ε is the strain tensor and θ represents a given set of model parameters defining structural parameters (material, geometry, etc.). Moreover, the space of admissible displacements $U(\bar{u})$ and admissible stresses $S(\bar{f})$ is defined by:

$$\begin{cases} U(\bar{u}) = \{u(z, t) \text{ s.r.} \mid u(z, t) = \bar{u} \text{ for each } z \in \partial_u \Omega \text{ and } u(z, 0) = u_0, \dot{u}(z, 0) = \dot{u}_0\} \\ S(\bar{f}) = \{\sigma(z, t) \text{ s.r.} \mid \sigma(z, t) \cdot n = \bar{f} \text{ for } z \in \partial_f \Omega\} \end{cases} \quad [1.3]$$

where “s.r.” designates functions that are sufficiently regular, defined on the confined stress and the kinetic energy for $u(z, t)$ and integrable squared for $\sigma(z, t)$, and n is the normal vector on the surface ∂f .

The problem is said to be *well-posed* in the sense of Hadamard [BUI 93] if, and only if, the three following conditions are verified:

- 1) a solution $u(z, t)$ exists $\forall z \in \Omega, \forall t \in [0, T]$ for \bar{u} and \bar{f} given;
- 2) the solution $u(z, t)$ is unique;
- 3) the solution permanently depends on \bar{u} and \bar{f} .

In particular, this posture requires $\partial \Omega = \partial \Omega_u \cup \partial \Omega_f$ and $\partial_u \Omega \cap \partial_f \Omega = \emptyset$ (see Figure 1.2). In this description, the direct problem will generally be *ill-posed* for at least two reasons:

– the presence of overdetermined data \bar{u} and \bar{f} in $\partial_{fu}\Omega$ generally leads to the inexistence of the solution, with the exception of the instance where \bar{u} and \bar{f} are compatible with the constitutive relation [1.2];

– the lack of data in a certain area of the boundary $\partial_0\Omega$ can lead to non-unicity. This is particularly the case when $\partial_{fu}\Omega = \emptyset$. In this instance, prescribing boundary data on force or displacement on $\partial_0\Omega$ makes the problem well-posed.

In our case, we are aiming to find the set of model parameters θ and the solution field u satisfying the equations of a model [1.1] and [1.2] above, which better represent the available data. Because the available data \bar{u} and \bar{f} can be noisy and overdetermined, just as the equations of the inexact model in comparison to the real physics (discretization of the area, material, etc.), the solution of this inverse problem could often be ill-posed in Hadamard's sense as it cannot comply with one or many of the conditions listed above.

In the field of solid mechanics, various authors have studied the identification of the model's properties based on observed data. To give an example, it has been shown in [BON 05] that, in the elastic example, the problem of finding a field of properties distributed $E(z)$ in the entire space Ω is an ill-posed problem in Hadamard's sense and it becomes necessary to introduce *a priori* knowledge, which draws near the solution.

There are various methods that exist for solving problems related to identifying a model's properties, depending on the nature of the problem (static, dynamic, available data, etc.). The identification problem generally ends up being formulated as an optimization problem, namely researching the minimum of a cost function that quantifies the difference between a model forecast and the available data to some extent.

Among the different approaches that exist for building a suitable cost, the following families can be distinguished:

– the least squares approach [TAR 82] where the difference between the data and the solution of the direct model projected on the observation space is measured with an L2 regulation;

- an approach based on auxiliary fields. In linear mechanics, the Maxwell–Betti reciprocity theorem and the cost functions are generally constructed on the overdetermined data on the boundary area. An interesting example of using this approach can be found in [AND 97] for detecting fissures on the inside of an elastic body;

- an approach consisting of these functional functions with an energy base, and in particular those based on the error in the constitutive relation for which a detailed description is given further on.

On the other hand, if the identification problem is ill posed, it will generally lead to the solution becoming sensitive or unstable against the noisy data. In order to overcome this problem, we will distinguish two classical approaches:

- Tikhonov’s regularization techniques [TIK 77], which are largely used and where an additional term is introduced into the aforesaid cost functions. This term represents an *a priori* knowledge of the solution being searched for and the property of stabilizing the results with regard to the noise in the data;

- the probabilistic approaches [TAR 05, ARN 07] where the uncertainties of the data and the model are quantified with the help of a stochastic framework, and a probability density function for the unknown parameters is generally searched for.

1.3. Identification of the strain hardening law

Some authors [GAV 96, MAH 97, GH0 98, YOS 98, YOS 03, DIO 03] have instigated a new approach within the context of identifying plastic behavior. In one research paper, the authors proposed to extend the sphere of classical testing analysis by carrying out a shift of measured response and a response simulated by finite elements. This method enables one to take some of the material or structure’s effects into consideration.

In [SCH 92], Schnur and Zabaraz were among the first to have attempted to overcome the homogeneity hypothesis by coupling a calculation code by finite elements with an optimization method in order to identify a material’s behavior. This inverse method, which consists of using an iterative process to minimize the gap between the simulation and the experience, has not stopped being developed over the last few years.

In [GAV 96], Gavrus *et al.* applied an inverse method to identify the rheological behavior of a thermoviscoplastic material subjected to a tensile and torsional stress in severe strain conditions, close to those attained for industrial applications. These authors developed an algorithm that couples the finite elements method, by simulating the test, with an optimization module. The objective function, which is formulated in the sense of least squares and shows the difference between the simulated and experimental measurements, is minimized by using the Gauss–Newton procedure.

In [MAH 96], Mahnken and Stein factored in local displacement measurements into the cost function to be minimized. They carried out a traction test on a flat steel test tube notched into its place. The image correlation method was then used to measure the displacement fields next to the notch. The strain hardening parameters and the elastic limit of the two elastic-plastic behavioral laws proposed were identified by minimizing the gap between the measurements and the simulation. To solve the minimization problem, the analytically calculated gradient method was used.

In [MEU 98], Meuwissen *et al.* identified plasticity models by using heterogeneous flat tests. The cost function to be minimized was the quadratic gap concerning the applied force and the displacement field, in the areas where the gradients were significant, experimentally simulated and measured. The authors used weighting coefficients in the cost function in order to take the measurement errors and the parameter dispersion into account. To minimize the cost function, a Gauss–Newton type method of the first order was then used. The gradient was calculated using finite differences.

In [KAJ 04], Kajberga *et al.* performed tensile tests on notched flat test tubes. To facilitate localizing the plasticity, they carried out their tests until the test tubes fractured. The speckle interferometry method was used to measure the displacement fields. The cost function was chosen as the difference between the values issued from the simulation and the experimental tests. Finally, the optimization problem was solved using a simplex method.

The general idea of these inverse methods, which combine simulation results and experimental measurements, remains the same for all the above authors. The difference is shown in the choice of optimization methods. One mainly finds the largest slope method, the conjugated gradient method, the quasi-Newton method, the Gauss–Newton method and the Levenberg–

Marquart method. For these methods, it is necessary to calculate the gradient of the objective function against the parameters to be identified. Usually, the finite differences, semianalytic or analytic derivation techniques are used. For zero-order optimization methods, like the simplex method and genetic algorithms, one does not have to calculate the gradient, as successive assessments of the objective function suffice.

1.3.1. Example of an application

In this section, we are focusing on the hydroforming of sheet metal. We will start with the tensile test and finish with the hydroformed part [RAD 16].

Assuming that the hardening on the sheet metal is purely isotropic, a single scalar parameter is necessary for describing the evolution of the surface run-off. This is the equivalent plastic strain that we calculated as being the integral time of the equivalent plastic strain rate: $\varepsilon = \int_0^T \dot{\varepsilon} dt$.

The evolution of the couple's surface level $(\sigma_y, \bar{\varepsilon}^p)$ is considered by means of the Swift hardening law:

$$\sigma_y = k(\varepsilon_0 + \bar{\varepsilon}^p)^n \quad [1.4]$$

where k is the hardening coefficient, ε_0 is the reference plastic strain and n is the strain hardening coefficient.

These three parameters are the material's characteristics. Three other parameters are not represented by the strain hardening model, but they affect the strain characteristics. They are the material's anisotropic parameters, the friction coefficient between the tools and the sheet metal and the thickness e of the sheet metal.

The parameters (k, ε_0, n) are calculated so that the constitutive equations, which are associated with the plastifying surface, reproduce the material's formatting characteristics at best. The problem that remains to be solved consists of finding the best combination of parameter damage that reduces the difference between the digital forecasts and the experimental results to a minimum.

This minimization is related to the differences between the experimental measurements of the stresses and their digital forecasts carried out on the tensile test tubes. Due to the complexity of the formulas used, a digital minimization strategy has been developed based on Nelder–Mead’s simplex method [FLE 87].

The technique for identifying the material’s parameters is based on the coupling between Nelder–Mead’s simplex method (Matlab[®] code) and the digital simulation according the finite elements method via Abaqus/Explicit[®] of the hydroforming [RAD 11]. To obtain information on the Abaqus/Explicit[®] the output file, one uses the advanced Python code (see Figure 1.3).

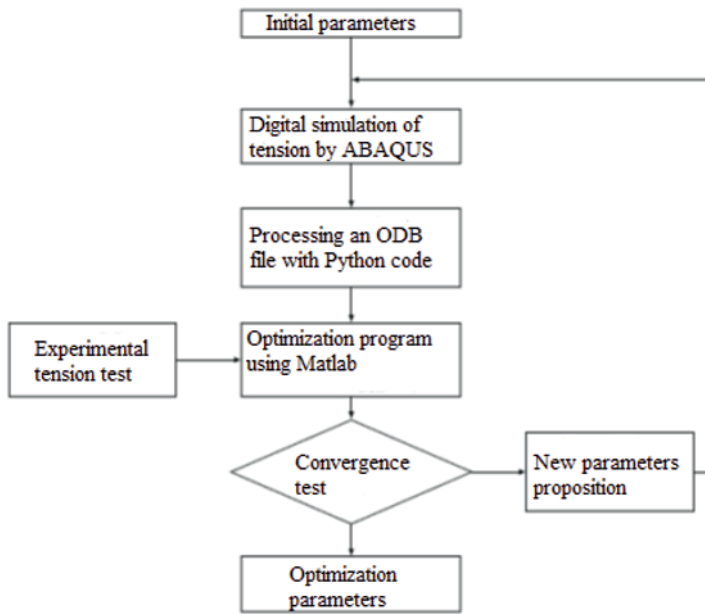


Figure 1.3. Identification process

1.3.2. Validation test

A finite element analysis has been carried out in three dimensions using the Abaqus/Explicit[®] finite elements code to study the hydroforming process [RAD 16]. One starts with the tensile test. Some rectangular samples in stainless steel have been manufactured with the following geometric characteristics (Figure 1.4): thickness $e = 1.0$ mm, width $l = 12.52$ mm and initial length $L = 100$ mm.

All the digital simulations were carried out under controlled displacement conditions with the constant speed $v = 0.1$ mm/s. The foreseen forces with respect to the displacements in comparison with the experimental results according to the three orientations studied are shown in Figure 1.4. With the small ductility (step 1), the maximum stress is around 360 MPa and reaches 25 % of the plastic strain. The final fracture is obtained for 45 % of the plastic strain. With the moderate ductility (step 3), the maximum stress is around 394 MPa and reaches 37.2 % of the plastic strain, the final fracture is obtained for 53 % of the plastic strain.

The best values of the material's parameters have been summarized in Table 1.1 with the help of the optimization procedure. At the heart of these coefficients, the response (stress vs. plastic strain) presents a nonlinear isotropic hardening with a maximum stress reached for plastic strains and the final fracture is obtained for 22 % of the plastic strain. The plastic strain of the optimal case is shown in Figure 1.4.

Step	Critical plastic strain (%)	k [MPa]	ε_0	n
1	25.8	381.3	0.0100	0.2400
2	29.8	395.5	0.0120	0.2415
3	37.2	415.2	0.0150	0.2450
Optimal	36.8	416.1	0.0198	0.2498

Table 1.1. Properties of the material used

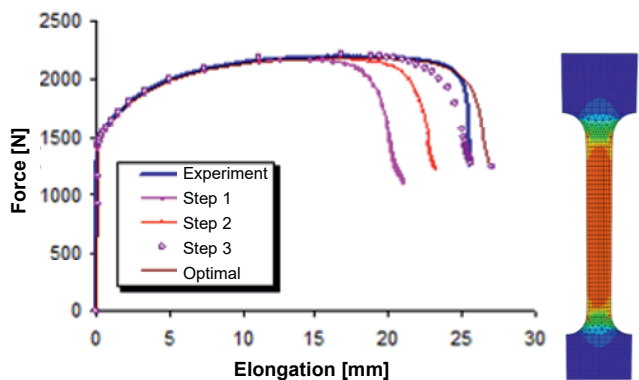


Figure 1.4. Force/elongation for different optimization steps and plastic strain map.
For a color version of this figure see, www.iste.co.uk/elhami/dynamics.zip

1.3.3. Hydroforming a welded tube

In this instance, the strain with the geometric singularities found in the welded tube is assumed to be transversally orthotropic, while its behavior is represented by the Swift model. A microscope is used to observe the transversal section of the wall to construct a geometric profile of the notch produced by the welded joint [AYA 11].

By considering the hypotheses related to an isotropic thin hull ($R=1$) with a uniform thickness, the established relations [RAD 16] allow the first experimental hardening model to be constructed using the internal/radial displacement pressure measurements. This is then proposed as an initial solution to solve the inverse problem of the necessary hardening law that minimizes the following objective function:

$$\xi_F = \frac{1}{m_p} \sqrt{\sum_{i=1}^{m_p} \left(\frac{F_{\text{exp}}^i - F_{\text{num}}^i}{F_{\text{exp}}^i} \right)^2} \quad [1.5]$$

where F_{exp}^i is the experimental value of the thrust force corresponding to its i st depth of nano-indentation H_i , F_{num}^i is the corresponding simulated thrust force and m_p is the total number of experimental points.

Different run-off stress evolutions of isotropic hardening (initial, intermediate and optimal) are proposed in order to estimate the best strain behavior with the geometric singularities found in hydroforming the tube.

Figures 1.5 and 1.6 represent the effective stress according to the plastic strain and the displacement/radial associated pressure for these three cases. As we can see, there is a strong correlation between the optimal hardening evolution and the experimental results. Table 1.2 summarizes the parameters of these models.

The anisotropy factor R is only determined for the evolution of the optimal hardening. The digital iterations have been performed on the hydroforming of the tube on the thickness's non-uniformity and the results obtained are shown in Figure 1.7. If R corresponds to the value of 0.976, one notices a strong improvement in the quality of the predicted results.

Model	ϵ_0	k (MPa)	n
Initial	0.025	1124.6	0.2941
Intermediate	0.055	692.30	0.2101
Optimal	0.080	742.50	0.2359

Table 1.2. Swift parameters of the different hardening evolutions

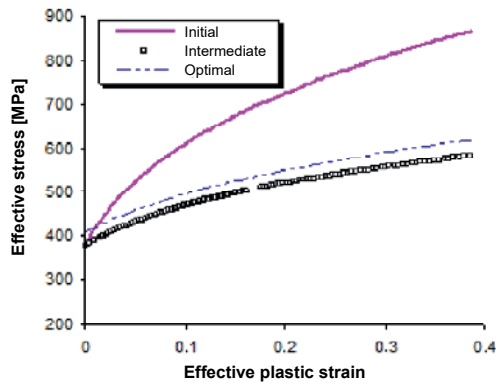


Figure 1.5. Stress–strain evolution for the different hardening laws. For a color version of this figure see, www.iste.co.uk/elhami/dynamics.zip

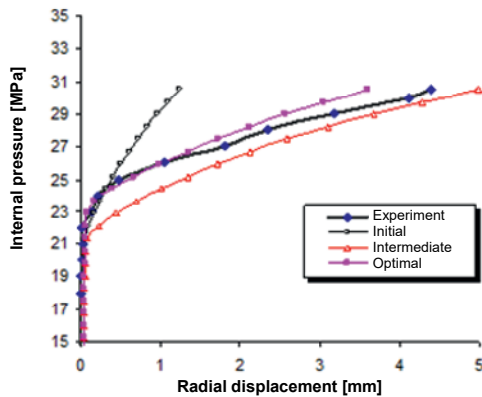


Figure 1.6. Internal pressure according to the radial displacement. For a color version of this figure see, www.iste.co.uk/elhami/dynamics.zip

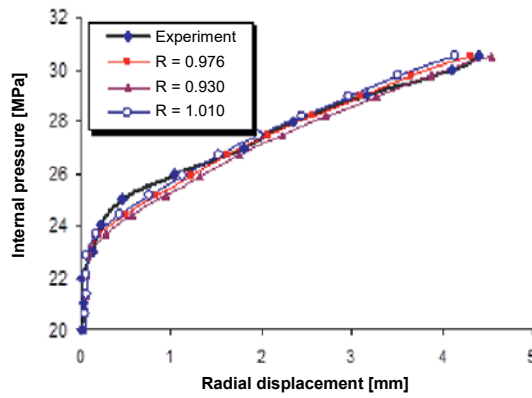


Figure 1.7. Radial displacement for different values of the anisotropy coefficient R . For a color version of this figure see, www.iste.co.uk/elhami/dynamics.zip

